RAFT-Mediated Emulsion Polymerization-Induced Self-Assembly for the Synthesis of Core-Degradable Waterborne Particles

Paul Galanopoulo, Noémie Gil, Didier Gigmes, Catherine Lefay, Yohann Guillaneuf, Maëlle Lages, Julien Nicolas, Franck d'Agosto, Muriel Lansalot

RESEARCH ARTICLE

RAFT-mediated emulsion polymerization-induced self-assembly for the synthesis of core-degradable waterborne particles

Paul Galanopoulo,[a] Noémie Gil,[b] Didier Gigmes,[b] Catherine Lefay,[b] Yohann Guillaneuf,[b] Maëlle Lages,[c] Julien Nicolas,[c] Franck D'Agosto,[a],* Muriel Lansalot[a],*

[a] Dr. P. Galanopoulo, Dr. M. Lansalot, Dr. F. D'Agosto Univ Lyon, Université Claude Bernard Lyon 1, CPE Lyon, CNRS, UMR 5128, Catalysis, Polymerization, Processes and Materials (CP2M), 43 Bd du 11 novembre 1918, 69616 Villeurbanne, France.
E-mail: muriel.lansalot@univ-lyon1.fr; franck.dagosto@univ-lyon1.fr
[b] Dr. N. Gil, Dr. D. Gigmes, Dr. C. Lefay, Dr. Y. Guillaneuf, Aix Marseille Univ, CNRS, Institut de Chimie Radicalaire, UMR 7273, Marseille, France.
[c] Dr. M. Lages, Dr. J. Nicolas, Université Paris-Saclay, CNRS, Institut Galien Paris-Saclay, 91400 Orsay, France

Supporting information for this article is given via a link at the end of the document.

Abstract: Poly(*N*-acryloylmorpholine) (PNAM)-decorated waterborne nanoparticles comprising a core of either degradable polystyrene (PS) or poly(*n*-butyl acrylate) (PBA) were synthesized by polymerization-induced self-assembly (PISA) in water. A PNAM bearing a trithiocarbonate chain end (PNAM-TTC) was extended *via* reversible addition-fragmentation chain transfer (RAFT)-mediated emulsion copolymerization of either styrene (S) or *n*-butyl acrylate (BA) with dibenzo[c,e]oxepane-5-thione (DOT). Well-defined amphiphilic block copolymers were obtained. The *in situ* self-assembly of these polymers resulted in the formation of stable nanoparticles. The insertion of thioester units in the vinylic blocks enabled their degradation under basic conditions. The same strategy was then applied to the emulsion copolymerization of BA with DOT using a poly(ethylene glycol) (PEG) equipped with a trithiocarbonate end group, resulting in PEG-decorated nanoparticles with degradable PBA-based cores.

Introduction

The development of new synthetic pathways for the production of degradable polymers has attracted increasing interest as these products found applications ranging from the synthesis of more environmental friendly and reusable materials[1–3] to applications in biomedicine.[4,5] The development of radical ring-opening polymerization (rROP) through the use of cyclic ketene acetals (CKAs) has given access to facile synthesis of ester-containing vinylic copolymers.[6,7] When comprising only a few ester units, these copolymers display properties similar to the ones of the vinylic homopolymers, but with the ability to be broken down into small oligomers by cleavage of the ester functions scattered along the backbone.[5,7,8] The use of CKAs for the synthesis of degradable vinylic polymers has however been restrained because of their relatively low reactivity toward common vinylic monomers and because they tend to hydrolyze rapidly even in mild conditions.[9] As a result, CKAs have been hardly employed in radical polymerization in aqueous dispersed media despite its industrial significance. Thionolactones have recently emerged as an appealing alternative to CKAs and more specifically dibenzo[c,e]oxepane-5-thione (DOT). The groups of Roth and Gutekunst reported that DOT was able to sustain a radical ring-opening mechanism to afford in-chain thioesters.[10–13] It was notably shown that its copolymerization with acrylates[10,13] and styrene (S)[14] led to random copolymers containing scattered in-chain thioester functions. Those polymers could then be degraded upon cleavage of the thioesters under the action of a strong base. The major interest of DOT comparing to CKAs is that it is not subjected to hydrolysis and is thus much easier to use in aqueous dispersed media. Indeed, while only two references dealt with the copolymerization of CKAs in aqueous dispersed media after 40 years of development,[15,16] our group was able to establish the emulsion copolymerization of DOT with S and *n*-butyl acrylate (BA)[17] only a couple of years after the radical (co)polymerization of thionolactones was established.[10,13]

In parallel to this work,[17] we investigate emulsion polymerization-induced self-assembly (PISA) mediated by reversible addition-fragmentation chain transfer (RAFT)[18–20] for the synthesis of core-degradable polymer particles. PISA involves the simultaneous synthesis and self-assembly of amphiphilic block copolymers using a controlled polymerization process. When performed in water, either by dispersion or emulsion, reversible-deactivation radical polymerization (RDRP) techniques can easily be used to generate waterborne self-stabilized nanoparticles, sometimes in high concentrations.[18,21,22] Nanoparticles obtained by PISA offer a wide range of applications ranging from biomedical applications to Pickering emulsion stabilizer and coatings. The combination of PISA with rROP (rROPISA) to synthesize self-stabilized nanoparticles made of a degradable vinylic polymer has already been established using RAFT.[23,24] Nonetheless, this technique has only been applied to polymerization in organic dispersed media and still requires additional steps to transfer the nanoparticles in aqueous phase. Very recently, however, taking advantage of the hydrolytic stability of DOT and its successful use in emulsion,[17] poly(acrylic acid) chains obtained by nitroxide mediated polymerization were used to initiate copolymerization of DOT with S or BA in water and generate nanoparticles by PISA.[25] Nevertheless, the reinitiation was not quantitative and a large amount of PAA chains did not participate in the formation of the block copolymer particles. In nanomedicine applications, the identification of a system that would lead to a complete consumption of the hydrophilic chains is required. In addition, the use of biocompatible hydrophilic chains is a prerequisite.

We identified that a macromolecular chain transfer agent (macroCTA) of poly(*N*-acryloylmorpholine) (PNAM), easily

accessible by RAFT, could be an interesting candidate as both non-ionic and biocompatible. Indeed, even though PNAM is far less common than poly(ethylene glycol) (PEG) in biomedical applications, it exhibits similar biocompatibility to PEG,[26,27] and PNAM-stabilized aggregates were shown to display equivalent biocompatibility to PEG-stabilized counterparts.[28] Besides, PNAM macroCTA has already proved to be an efficient stabilizing block in the formation of polystyrene and poly(vinyl acetate) particles by emulsion PISA.[29–31] MacroCTA of PNAM is thus used for the RAFT-mediated emulsion copolymerization of either styrene or *n*-butyl acrylate with DOT (Scheme 1). To show the versatility of the process, the same approach is then applied to the emulsion copolymerization of BA with DOT using a PEG-based macroCTA.

Results and Discussion

A PNAM bearing a trithiocarbonate chain-end (PNAM-TTC) was first synthesized by RAFT solution polymerization according to a previously established protocol (see supporting information),[30] to obtain a well-defined hydrophilic PNAM macroCTA of ca. 26 units ($M_{n,MALDI}$ = 3910 g mol^{-1}, $Đ$ = 1.07*)*.

PNAM-TTC mediated aqueous emulsion (co)polymerization of BA or S with DOT were performed according to our previous studies.[29,30] The syntheses were performed targeting a solid content of about 10 wt% and using 4,4′-azobis(4-cyanopentanoic acid) (ACPA) as initiator (Scheme 1). The ratio between the concentration of macroCTA and initiator was maintained to 4.5 to limit the fraction of dead chains. Two preliminary syntheses were performed with the aim of polymerizing BA or S alone (PNAM-BA and PNAM-S, Table 1) before adding about 2 mol% of DOT (PNAM-BA-DOT and PNAM-S-DOT, Table 1) so that the concentration of DOT is set just below its solubility limit.[17] We targeted a degree of polymerization (DP_n) of about 200 for the hydrophobic block as it should allow introducing enough DOT units to have a noticeable degradability (4 DOT units on average for f_{DOT} = 2 mol% and DP_n = 200). RAFT-mediated emulsion polymerization of BA in presence of a PNAM macroCTA, that has not yet been reported, led to full conversion of BA and a stable latex. A stable latex was also obtained in the presence of DOT (Figure S5), and in both experiments full conversion of BA was achieved in less than 2 h. The (co)polymerization of DOT and styrene did also lead to stable latexes and full conversion of styrene.

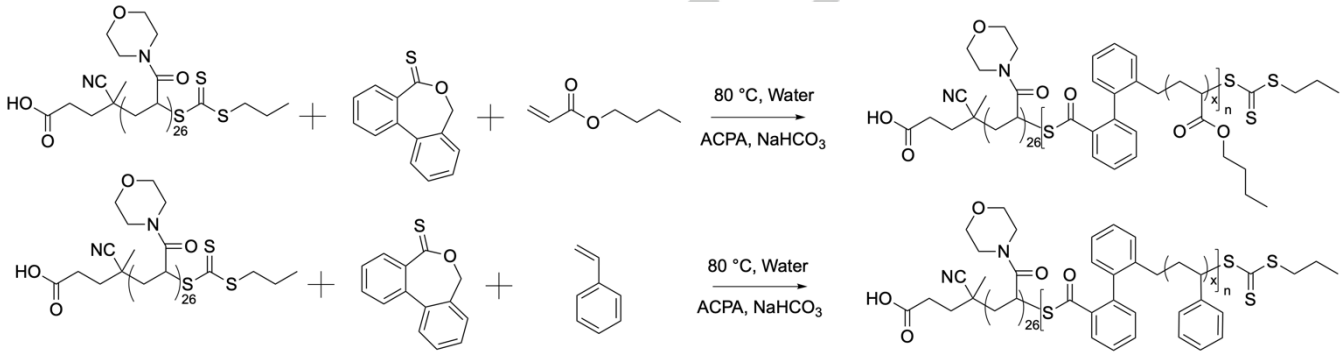

Scheme 1. Emulsion copolymerization of DOT with BA or S in the presence of PNAM-TTC.

Table 1. Experimental conditions and results for the PNAM-TTC mediated emulsion (co)polymerization of BA or S with DOT.

Expt.	$DP_{n,target}$[a]	f_{DOT}[b] (%)	τ_s th [c] (%)	t (h)	τ_s[c] (%)	Conv.[d] (%)	M_n th [e] (kg mol^{-1})	M_n [f] (kg mol^{-1}) $Đ$	M_n^{deg} [f] (kg mol^{-1}) $Đ$	Z_{ave}[g] (nm) PDI	D_n[h] (nm) D_w/D_n
PNAM-BA	199	0.0	9.8	2	9.6	98	28.6	21.6 1.4	23.4 1.6	65 0.16	45 1.08
PNAM-BA-DOT	202	1.8	10.1	2	10.1	100	29.5	22.7 1.3	5.6 1.7	65 (+633)	47 1.07
PNAM-S	199	0.0	9.9	4	10	98	24.2	19.8 1.3	21.0 1.4	48 0.13	40 1.03
PNAM-S-DOT	206	2.0	10.1	3.7	10	95	24.4	20.0 1.2	5.9 1.9	51 (+410)	41 1.04

Experimental conditions: 80 °C, [PNAM-TTC]/[ACPA] = 4.5, [$NaHCO_3$]/[ACPA] = 3.5. [a] The targeted degree of polymerization is defined by the experimental ratio: ([monomer]+[DOT])/[PNAM-TTC], the monomer being either BA or styrene. [b] Molar fraction of DOT in the initial monomer mixture. [c] Theoretical solid content (τ_{th}) and experimental final solid content (τ_s) measured by gravimetric analysis. [d] Conversion of BA or styrene calculated by gravimetric analysis. [e] Theoretical number-average molar mass of the block copolymer calculated using the conversion and the targeted DP_n. [f] Experimental number-average molar mass, M_n, and dispersity, M_w/M_n, of the copolymer or degradation product determined by SEC-THF using a calibration based on PS standards. [g] Intensity-average diameter and polydispersity index of the final particles from DLS. [h] Number-average diameter and dispersity index determined by statistical analysis of the cryo-TEM images.

DLS results showed that in the case of DOT-free syntheses, the latexes PNAM-BA and PNAM-S (Table 1) were composed of particles of about 65 nm and 48 nm, respectively. These sizes are consistent with the successful formation and self-assembly of PNAM-*b*-PBA and PNAM-*b*-PS block copolymers. When adding DOT to the recipe, a second population with a diameter 10 times higher was detected by DLS. The number-size distribution given by the DLS measurement nevertheless reveals that large particles are present in a negligible fraction compared to the smaller ones (Figures S4). Indeed, the concentration of these large objects should be very low for DLS to still detect particles that possess a diameter 10 times smaller.

Additionally, no large particles were detected in any of the (cryo-)TEM images obtained from latex PNAM-BA-DOT (Figure 1) and PNAM-S-DOT (Figure 2). Thus, the sizes measured from the (cryo-)TEM were found to be almost identical for latexes obtained from the polymerization of the vinyl monomer with or without DOT (D_n = 45 nm for PNAM-BA and D_n = 47 nm for PNAM-BA-DOT, D_n = 40 nm for PNAM-S and D_n = 41 nm for PNAM-S-DOT, Table 1) with narrow size-distributions in all cases (Figures 1 and 2).

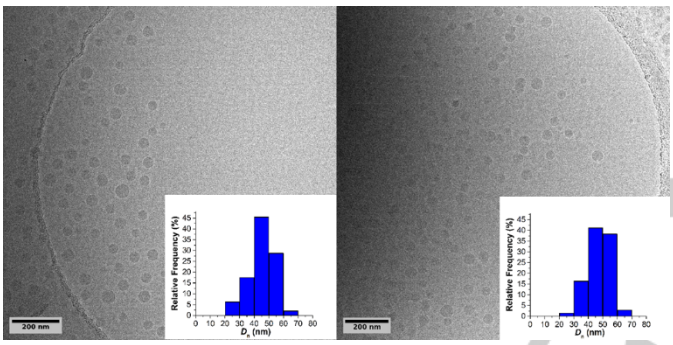

Figure 1. Representative cryo-TEM images of crude latexes PNAM-BA (left, D_n = 45 nm, D_w/D_n = 1.08) and PNAM-BA-DOT (right, D_n = 47 nm, D_w/D_n = 1.07) with corresponding size distribution. Size distributions were calculated on an average of 200 particles.

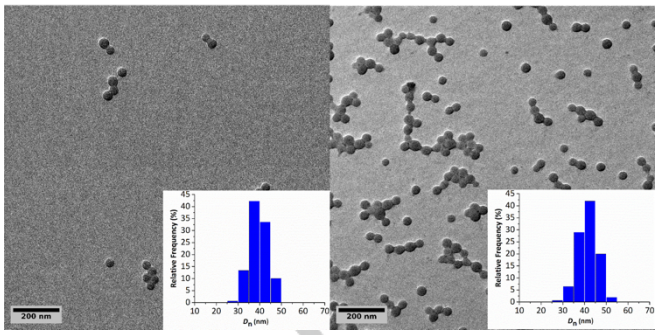

Figure 2. Representative TEM images of crude latexes PNAM-S (left, D_n = 40 nm, D_w/D_n = 1.03) and PNAM-S-DOT (right, D_n = 41 nm, D_w/D_n = 1.04) with corresponding size distribution. Size distributions were calculated on an average of 150 particles.

While in the case of BA homopolymerization full conversion was reached in less than 40 min, it took nearly 80 min to fully convert BA in the presence of DOT (Figure 3. a). DOT also proved to be polymerized at a faster rate than BA resulting in composition drift as showed by the decreasing average number of DOT units in the copolymer (F_{DOT}) along the reaction in experiment PNAM-BA-DOT (Figure 3. b). This is consistent with our previous observations in conventional emulsion (co)polymerization where the observed compositional drift led to the formation of chains with different contents of DOT units.[17] However, the present systems rely on a RDRP technique. All the chains are thus homogeneous in composition and the P(BA-*co*-DOT) segments are expected to be gradient copolymers incorporating less and less DOT units upon BA conversion, *i.e.* upon the hydrophobic block growth.[32]

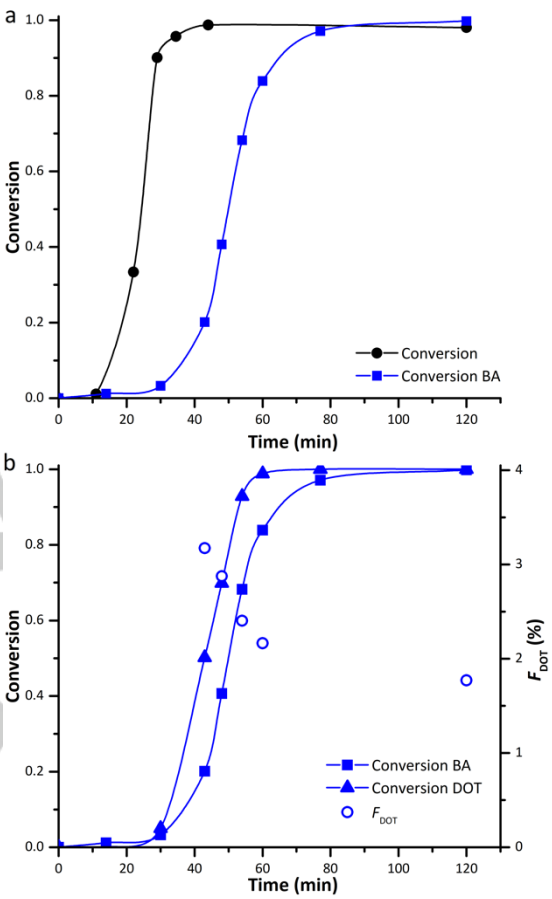

Figure 3. RAFT-mediated (co)polymerization of BA with DOT in the presence of PNAM-TTC (Table 1). a) Evolution of BA conversion *versus* time for experiment PNAM-BA (black circles) and PNAM-BA-DOT (blue squares). b) Evolution of BA conversion (squares), DOT conversion (dashes) and average molar fraction of DOT in the copolymers (F_{DOT}, open circles) *versus* time for experiment PNAM-BA-DOT.

In the case of the (co)polymerization of S, full conversion was achieved within about 2 h after an inhibition period of about 1 h, whether DOT was present or not (Figure 4.). Like in the copolymerization of DOT with S under conventional emulsion conditions, DOT did not induce any retardation on the polymerization of S under rROPISA conditions.[17]

SEC analysis confirmed the good control of the polymerization for each experiment, with and without DOT (Figure 5. and **Figure 6.** , for the DOT containing systems, Figures S7 and S8 for the two others).

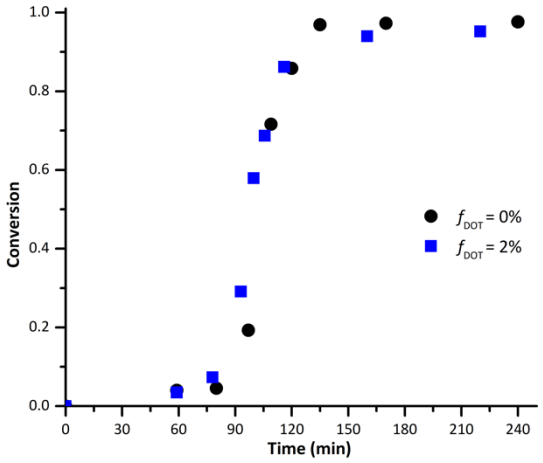

Figure 4. Evolution of S conversion *versus* time for experiments PNAM-S (circles) and PNAM-S-DOT (squares, Table 1).

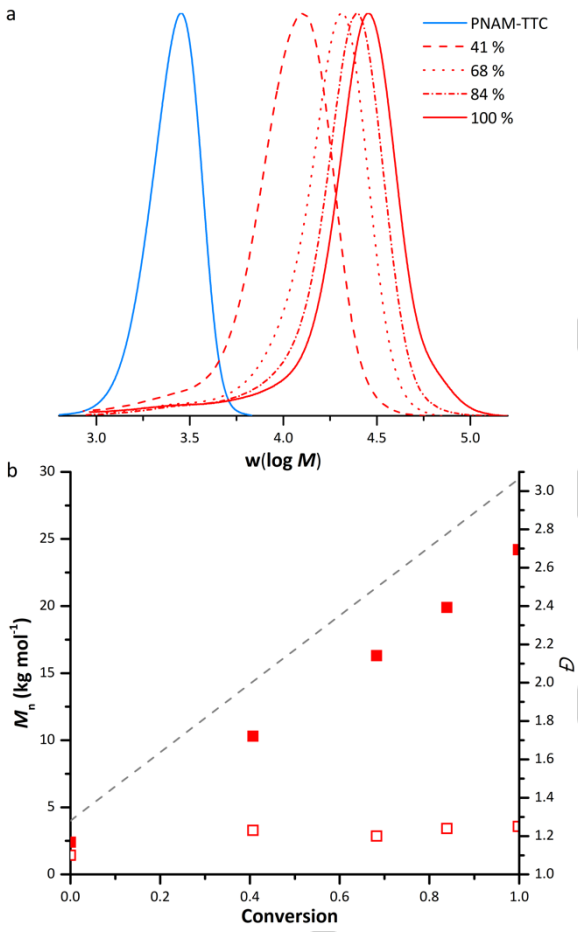

Figure 5. SEC-THF results for experiment PNAM-BA-DOT (Table 1). a) Molar mass distribution analysis for samples withdrawn depending on BA conversion. b) Evolution of the number-average molar mass M_n (plain squares) and dispersity ($Đ = M_w/M_n$, hollow squares) with BA conversion (the dashed line corresponds to the theoretical M_n values).

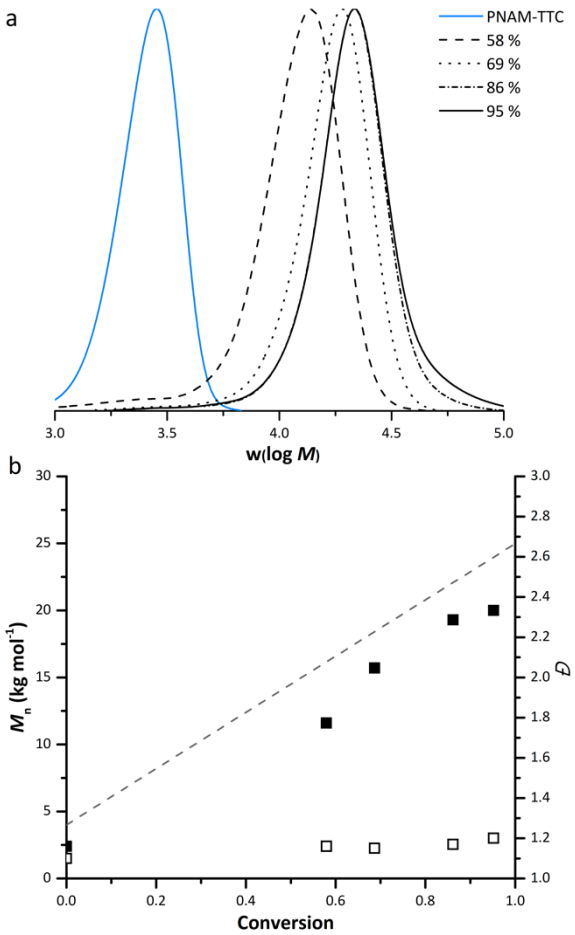

Figure 6. SEC-THF results for experiment PNAM-S-DOT (Table 1). a) Molar mass distribution analysis for samples withdrawn depending on styrene conversion. b) Evolution of the number-average molar mass M_n (plain squares) and dispersity ($Đ = M_w/M_n$, hollow squares) with styrene conversion (the dashed line corresponds to the theoretical M_n values)

The shift of the molar mass distributions (MMD) toward higher molar masses with increasing conversion, along with the absence of residual macroCTA attest for the good blocking efficiency, *i.e.,* all the PNAM chains were reinitiated to form diblock copolymers. Narrow MMDs were observed all along the synthesis in both cases as corroborated by the low dispersity values.

Eventually, molar masses increased linearly with the conversion in all cases (Figures 5, 6, S7 and S8). The measured number-average molar masses were nonetheless found to be lower than the expected ones. This is probably due to the use of the PS calibration, which proved to be relatively inadequate with PNAM[33] and is thus likely also inadequate for PNAM-based block copolymers. Overall, SEC analyses allowed attesting of the good control and the formation of well-defined block copolymers.

Thus, all data indicate that the obtained latexes are the product of a proper PISA mechanism.

Next, we were able to attest of the incorporation of the DOT units. ^{1}H NMR analysis was performed on the dried latexes. In the case of PNAM-BA-DOT, the incorporation of the thioester units is attested by the presence of the exact same signals between 7 and 8 ppm (protons *a*, *b*, *c* and *d* in Figure 7**.**) that were previously attributed to the aromatic protons of DOT units in the copolymers.[10,13,17] In the case of PNAM-S-DOT the presence of

thioester units in the copolymer was more difficult to assert. It is worth mentioning that no trace of residual DOT monomer can be spotted on the spectrum (signals expected at 5.2 and 8.2 ppm), implicitly indicating that DOT would have been entirely consumed. Yet, signals characterizing DOT units incorporated into the chains do not appear clearly in the ^{1}H NMR spectrum (**Figure 8.**). The signals of the aromatic protons of DOT units (over 7 ppm) are overlapped by those of S units (including those of residual amount of remaining S monomer). The signal at 4 ppm can be attributed to the proton of a S unit next to a thioester group[14,17] (**Figure 8.**). However, this signal overlapped partially with signals associated to PNAM units (from 3 to 4 ppm).

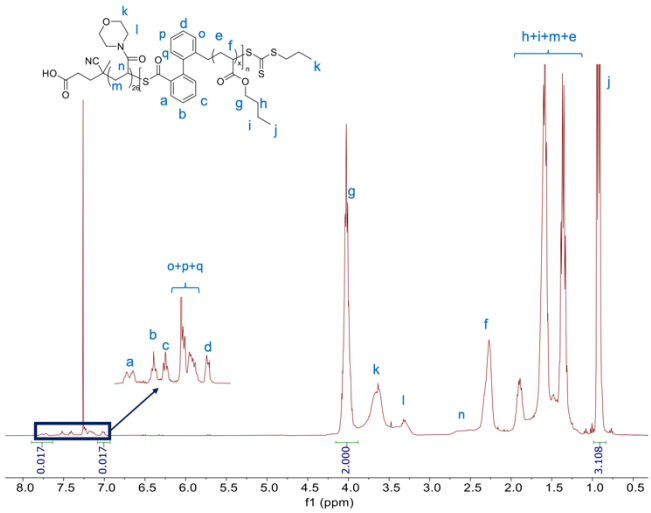

Figure 7. ^{1}H NMR spectrum of dried extract from the latex PNAM-BA-DOT (Table 1) with corresponding assignment ($CDCl_3$, 256 scans).

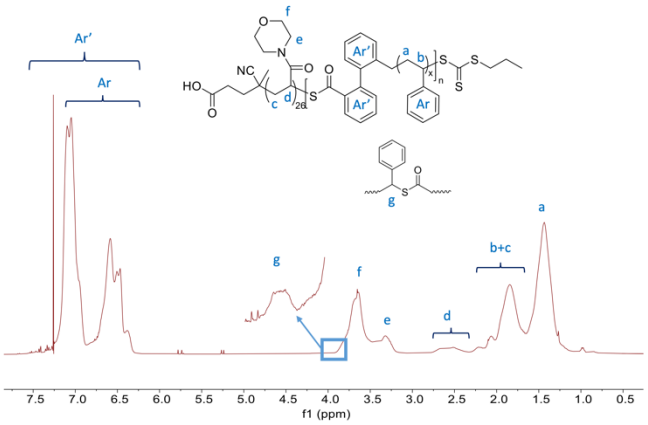

Figure 8. ^{1}H NMR spectrum of the dried extract from the latex PNAM-S-DOT (Table 1) ($CDCl_3$, 256 scans).

We eventually assessed the degradability of the P(BA-*co*-DOT) and P(S-*co*-DOT) blocks. The dry extracts obtained from experiments PNAM-BA, PNAM-BA-DOT, PNAM-S and PNAM-S-DOT were treated with 1,5,7-triazabicyclo[4.4.0]dec-5-ene (TBD), an organo-soluble base.[14,17] The treatment of PNAM-BA-DOT and PNAM-S-DOT induced a shift of the MMD toward the lower molar masses confirming the degradation of the copolymers (Figure 9.). Treatment with TBD yielded oligomers with a M_n of 5.6 kg mol^{-1} for PNAM-BA-DOT and 5.9 kg mol^{-1} PNAM-S-DOT, while the original copolymers presented a M_n of 22.7 kg mol^{-1} and 20.0 kg mol^{-1}, respectively (Table 1). An estimation based on the M_n values before and after degradation (which obviously do not account for chain-end effect on the SEC elution) indicate a 75% M_n loss for PNAM-BA-DOT and 71% for PNAM-S-DOT. Considering the molar mass of the non-degradable PNAM block, these M_n losses would increase to 84 and 80%, respectively.

MMD of the degraded polymers are broad (Figure 9). This might be the result of the formation of different populations, including the original PNAM carrying a few BA or S units, as well as oligomers resulting from the degradation of the P(BA-*co*-DOT) or P(S-*co*-DOT) blocks. Treatment of the dry extracts of experiments PNAM-BA and PNAM-S did not induce any significant shift of the molar mass (Table 1), confirming that degradation occurs through the cleavage of DOT units in the vinylic blocks.

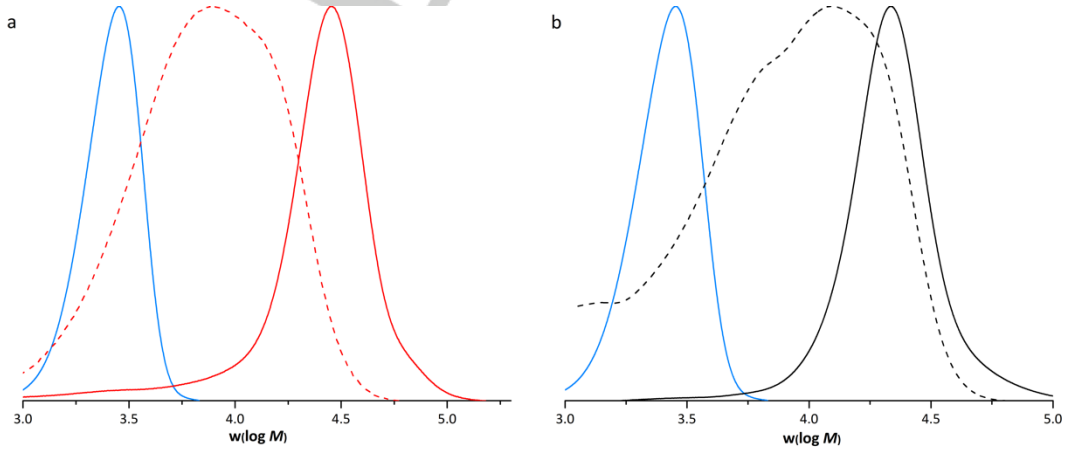

Figure 9. Molar mass distribution from SEC-THF analysis for a) latex PNAM-BA-DOT (plain red line) and b) PNAM-S-DOT (plain black line), their degradation product after treatment of the dry extract with TBD overnight (dashed line) and of PNAM-TTC (blue line).

We then investigated the synthesis of PEG-decorated particles to diversify the types of particles of potential biomedical interest. We first synthesized the appropriate PEG macroCTA with a trithiocarbonate end group (PEG-TTC) by esterification of a commercial PEG-OH and according to established results on the RAFT-mediated emulsion polymerization of BA (see supporting information).[34,35] This PEG-TTC (M_n = 3250 g mol^{-1}, $Đ$ = 1.05) was then employed in the RAFT-mediated emulsion copolymerization of BA with DOT (Table 2). We used the same conditions as for PNAM-mediated experiments, *i.e.,* targeting a DP_n of about 200 and a solid content of 10 wt%, adding a small fraction of DOT in BA (1.0 mol%, PEG-BA-DOT1). A control experiment was also performed in absence of DOT (PEG-BA). It is worth mentioning that the PEG-TTC-mediated emulsion copolymerization of DOT with S was also probed but led to poor control of the polymerization and colloidal stability issues.

Both reactions led to the formation of stable latexes. The presence of DOT in the medium once again proved to have a significant retarding effect on the polymerization of BA. While full BA conversion was reached in less than 2 h and at 70 °C in absence of DOT (PEG-BA, Table 2), it only reached 24% conversion after 4 h when copolymerizing with DOT (PEG-BA-DOT1, Table 2, Figure S9). The temperature was thus raised to 80 °C (while also increasing the amount of DOT to 1.6 mol%) to reach 85% BA conversion after about 4 h (PEG-BA-DOT2, Table 2). Kinetics showed once more that DOT was copolymerized at a faster rate than BA, resulting in the formation of a gradient copolymer for the vinylic block (see Figure S9). The polymerization showed good control as attested by the linear increase of the molar masses with the conversion and the shift of the MMD toward higher molar masses (Figure 10). The chromatograms also displayed residual signal in the region of the initial PEG-TTC. This probably accounts for non-functionalized PEG-OH as ^{1}H NMR analysis of PEG-TTC indicates that 85% of functionalization was reached (see supporting information, Figure S3). The number-average molar masses were consistently close to the expected ones considering a functionalization of 85% for the PEG-TTC (Table 2).

The incorporation of the thioester units was demonstrated by ^{1}H NMR spectroscopy analysis of the dried latex PEG-BA-DOT2, which shows the specific aromatic signals *a*, *b*, *c* and *d* (see supporting information, Figure S11). Additionally, this spectrum did not indicate any trace of remaining DOT monomer showing that it was entirely consumed during the polymerization.

Table 2. Experimental conditions and results for the PEG-mediated emulsion (co)polymerization of BA with DOT.

Expt.	$DP_{n,target}$[a]	f_{DOT}[b] (%)	τ_s th [c] (%)	T (°C)	t (h)	τ_s[c] (%)	Conv.[d] (%)	F_{DOT}[e] (%)	M_n th [f] (kg mol^{-1})	M_n [g] (kg mol^{-1}) $Đ$	M_n deg [g] (kg mol^{-1}) $Đ$	Z_{ave}[h] (nm) PdI
PEG-BA	207	0.0	10.2	70	4.2	9.8	95	-	32.2	34.8 1.3	33.5 1.5	229 0.03
PEG-BA-DOT1	209	1.0	10.2	70	4.2	3.3	24	2.5	10.1	n.d.	n.d.	n.d.
PEG-BA-DOT2	187	1.6	10.1	80	3.7	9.0	85	1.9	26.4	30.3 1.2	7.7 2.0	411 0.01

Experimental conditions: [PEG-TTC]/[ACPA] = 4, [$NaHCO_3$]/[ACPA] = 3.5. [a] The targeted degree of polymerization is defined by the experimental ratio: ([BA]+[DOT])/[PEG-TTC]. [b] Molar fraction of DOT in the initial monomer mixture. [c] Theoretical solid content (τ_{th}) and experimental final solid content (τ_s) measured by gravimetric analysis. [d] Conversion of BA calculated by gravimetric analysis. [e] Average molar fraction of inserted DOT in the resulting copolymers estimated by ^{1}H NMR. [f] Theoretical number-average molar mass of the block copolymer calculated using the conversion, targeted DP_n and acknowledging a functionalization of 85% for the PEG. [g] Experimental number-average molar mass, M_n, and dispersity, M_w/M_n, of the copolymer or degradation product determined by SEC-THF using a calibration based on PS standards. [h] Intensity-average diameter and polydispersity index of the final particles from DLS.

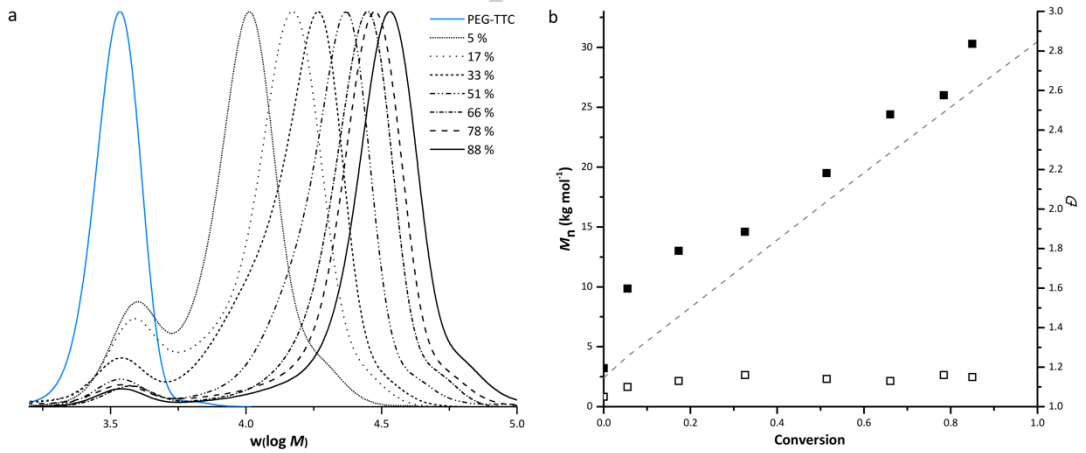

Figure 10. SEC-THF results for experiment PEG-BA-DOT2 (Table 2). a) Molar mass distribution analysis for samples withdrawn depending on BA conversion. b) Evolution of the number-average molar masses M_n (plain squares) and dispersity ($Đ = M_w/M_n$, hollow squares) with BA conversion (the dashed line corresponds to the theoretical M_n values for a 85% functionalized PEG macroCTA).

DLS results (Table 2) show that the obtained particles are much larger than those obtained in the case of PNAM-mediated PISA and, more generally, larger than what is expected in the case of emulsion PISA. Cryo-TEM images showed that spherical particles were obtained. Those particles however seem to contain “holes” (Figure 11). This phenomenon has been already observed in the case of polymerization of either BA or S using a PEG-based macroCTA.[35] The trapping of PEG chains inside the particles and formation of water-pools by analogy to similar results already obtained in emulsion polymerization was put forward as a possible explanation for the visualization of these holes.[36–38] Their formation would result from a poor stabilization ability of the PEG chains.

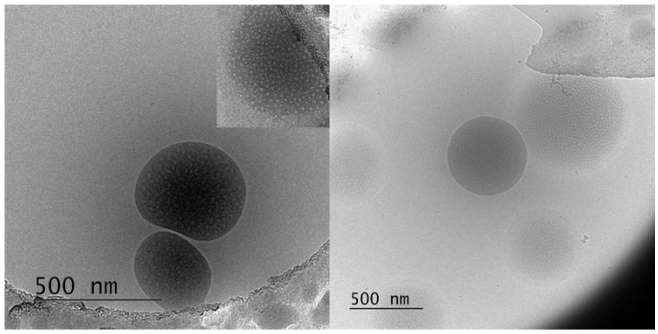

Figure 11. Representative cryo-TEM images of the crude latex PEG-BA (left) and PEG-BA-DOT2 (right).

Eventually, the dried extract obtained from PEG-BA-DOT2 (Table 2) was treated by TBD to assess the degradability of the chains. Molar mass distributions displayed a significant shift toward the lower molar masses in both cases confirming that those copolymers could be degraded (**Figure 12.**). The initial molar mass of the copolymer was found to be 30.1 kg mol^{-1} and was reduced down to 7.7 kg mol^{-1} after degradation. The dried extracts obtained from PEG-BA was also subjected to the treatment with TBD resulting in no significant loss of molar mass confirming that degradation occurs through the cleavage of DOT units in the PBA block.

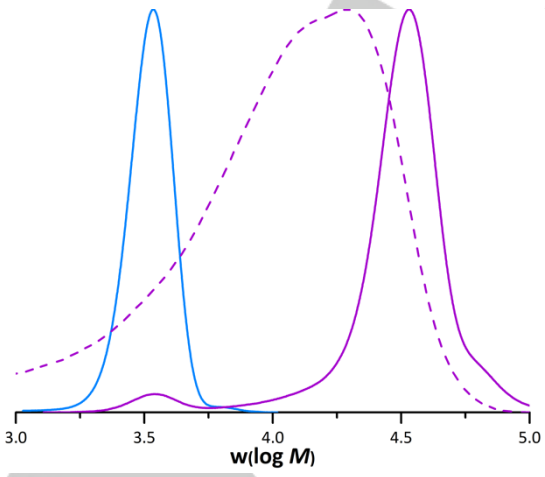

Figure 12. Molar mass distribution from SEC-THF analysis of the dry extract of latex PEG-BA-DOT2 (plain purple line), after treatment with TBD overnight (dashed line) and of PEG-TTC (blue line).

Conclusion

Trithiocarbonate-terminated PNAM or PEG were used as macroCTAs to mediate the aqueous emulsion copolymerization of either S or BA with DOT. The syntheses yielded very high conversions in rather short times and led to the formation of well-defined PNAM-*b*-P(S-*co*-DOT), PNAM-*b*-P(BA-*co*-DOT) and PEG-*b*-P(BA-*co*-DOT) amphiphilic block copolymers. Stable waterborne nanoparticles were formed by the *in situ* self-assembly of these block copolymers. Eventually, the hydrophobic blocks proved to be degradable *via* the cleavage of the thioester functions under basic conditions. Compared to the PEG-decorated nanoparticles, the PNAM ones can be obtained under a broader range of conditions and tolerate various hydrophobic monomers. This work establishes the first example of an efficient and simple pathway for the direct synthesis in water of nanoparticles with a shell made of a biocompatible polymer and a core made of degradable vinylic polymers. PISA in emulsion is not just a straightforward transposition of emulsion polymerization to the production of amphiphilic block copolymers, nor is the design of any kind of block copolymers by PISA. Indeed, it requires a fine tuning of the chemistry by the RAFT process with the physicochemical aspects of the system. Considering the interest raised by PISA in the recent years,[22] this type of nanoparticles and the way to make them should be considered as additional useful tools for the design of vehicles for drug delivery or nanomedicine applications.[4,39,40]

Acknowledgements

The authors acknowledge the financial support from the Agence Nationale de la Recherche (grant number ANR-18-CE06-0014 CKAPART). Pierre-Yves Dugas (CP2M) is acknowledged for the (cryo-)TEM observations.

Keywords: Degradable Polymers · PISA · Emulsion · Nanoparticles · Thionolactone

[1] *Nature* **2021**, *590*, 363–364.
[2] M. Häußler, M. Eck, D. Rothauer, S. Mecking, *Nature* **2021**, *590*, 423–427.
[3] B. Jothimani, B. Venkatachalapathy, N. S. Karthikeyan, C. Ravichandran, in *Green Biopolym. Their Nanocomposites* (Ed.: D. Gnanasekaran), Springer, Singapore, **2019**, pp. 403–422.
[4] V. Delplace, J. Nicolas, *Nat. Chem.* **2015**, *7*, 771–784.
[5] T. Pesenti, J. Nicolas, *ACS Macro Lett.* **2020**, 1812–1835.
[6] W. J. Bailey, Z. Ni, S.-R. Wu, *J. Polym. Sci. Polym. Chem. Ed.* **1982**, *20*, 3021–3030.
[7] A. Tardy, J. Nicolas, D. Gigmes, C. Lefay, Y. Guillaneuf, *Chem. Rev.* **2017**, *117*, 1319–1406.
[8] S. Agarwal, *Polym. Chem.* **2010**, *1*, 953–964.
[9] A. J. Kresge, T. S. Straub, *J. Am. Chem. Soc.* **1983**, *105*, 3957–3961.
[10] N. M. Bingham, P. J. Roth, *Chem. Commun.* **2019**, *55*, 55–58.
[11] N. M. Bingham, Q. un Nisa, S. H. L. Chua, L. Fontugne, M. P. Spick, P. J. Roth, *ACS Appl. Polym. Mater.* **2020**, *2*, 3440–3449.
[12] M. P. Spick, N. M. Bingham, Y. Li, J. de Jesus, C. Costa, M. J. Bailey, P. J. Roth, *Macromolecules* **2020**, *53*, 539–547.
[13] R. A. Smith, G. Fu, O. McAteer, M. Xu, W. R. Gutekunst, *J. Am. Chem. Soc.* **2019**, *141*, 1446–1451.
[14] N. Gil, B. Caron, D. Siri, J. Roche, S. Hadiouch, D. Khedaioui, S. Ranque, C. Cassagne, D. Montarnal, D. Gigmes, C. Lefay, Y. Guillaneuf, *Macromolecules* **2022**, *55*, 6680–6694.

[15] J. M. Siebert, D. Baumann, A. Zeller, V. Mailänder, K. Landfester, *Macromol. Biosci.* **2012**, *12*, 165–175.
[16] M. C. D. Carter, A. Hejl, S. Woodfin, B. Einsla, M. Janco, J. DeFelippis, R. J. Cooper, R. C. Even, *ACS Macro Lett.* **2021**, *10*, 591–597.
[17] P. Galanopoulo, N. Gil, D. Gigmes, C. Lefay, Y. Guillaneuf, M. Lages, J. Nicolas, M. Lansalot, F. D'Agosto, *Angew. Chem. Int. Ed.* **2022**, *61*, e202117498.
[18] F. D'Agosto, J. Rieger, M. Lansalot, *Angew. Chem. Int. Ed.* **2020**, *59*, 8368–8392.
[19] J. Wan, B. Fan, S. H. Thang, *Chem. Sci.* **2022**, *13*, 4192–4224.
[20] S. L. Canning, G. N. Smith, S. P. Armes, *Macromolecules* **2016**, *49*, 1985–2001.
[21] C. Liu, C.-Y. Hong, C.-Y. Pan, *Polym. Chem.* **2020**, *11*, 3673–3689.
[22] N. J. W. Penfold, J. Yeow, C. Boyer, S. P. Armes, *ACS Macro Lett.* **2019**, *8*, 1029–1054.
[23] E. Guégain, C. Zhu, E. Giovanardi, J. Nicolas, *Macromolecules* **2019**, *52*, 3612–3624.
[24] C. Zhu, S. Denis, J. Nicolas, *Chem. Mater.* **2022**, *34*, 1875–1888.
[25] M. Lages, N. Gil, P. Galanopoulo, J. Mougin, C. Lefay, Y. Guillaneuf, M. Lansalot, F. D'Agosto, J. Nicolas, *Macromolecules* **2022**, *55*, 9790–9801
[26] M. Gorman, Y. H. Chim, A. Hart, M. O. Riehle, A. J. Urquhart, *J. Biomed. Mater. Res. A* **2014**, *102*, 1809–1815.
[27] M. Bencini, E. Ranucci, P. Ferruti, A. Manfredi, F. Trotta, R. Cavalli, *J. Polym. Sci. A Polym. Chem.* **2008**, *46*, 1607–1617.
[28] V. P. Torchilin, V. S. Trubetskoy, K. R. Whiteman, P. Ferruti, F. M. Veronese, P. Caliceti, *J. Pharm. Sci.* **1995**, *84*, 1049–1053.
[29] J. Lesage de la Haye, X. Zhang, I. Chaduc, F. Brunel, M. Lansalot, F. D'Agosto, *Angew. Chem. Int. Ed.* **2016**, *55*, 3739–3743.
[30] I. Chaduc, E. Reynaud, L. Dumas, L. Albertin, F. D'Agosto, M. Lansalot, *Polymer* **2016**, *106*, 218–228.
[31] S. Binauld, L. Delafresnaye, B. Charleux, F. D'Agosto, M. Lansalot, *Macromolecules* **2014**, *47*, 3461–3472.
[32] D. Gigmes, P. H. M. V. Steenberge, D. Siri, D. R. D'hooge, Y. Guillaneuf, C. Lefay, *Macromol. Rapid Commun.* **2018**, *39*, 1800193.
[33] F. D'Agosto, R. Hughes, M.-T. Charreyre, C. Pichot, R. G. Gilbert, *Macromolecules* **2003**, *36*, 621–629.
[34] J. Rieger, F. Stoffelbach, C. Bui, D. Alaimo, C. Jérôme, B. Charleux, *Macromolecules* **2008**, *41*, 4065–4068.
[35] J. Rieger, G. Osterwinter, C. Bui, F. Stoffelbach, B. Charleux, *Macromolecules* **2009**, *42*, 5518–5525.
[36] H. Kobayashi, E. Miyanaga, M. Okubo, *Langmuir* **2007**, *23*, 8703–8708.
[37] W. Zhang, F. D'Agosto, O. Boyron, J. Rieger, B. Charleux, *Macromolecules* **2011**, *44*, 7584–7593.
[38] A. M. dos Santos, T. Le Bris, C. Graillat, F. D'Agosto, M. Lansalot, *Macromolecules* **2009**, *42*, 946–956.
[39] J. Nicolas, *Chem. Mater.* **2016**, *28*, 1591–1606.
[40] C. Zhu, J. Nicolas, *Biomacromolecules* **2022**, *23*, 3043–3080.

Entry for the Table of Contents

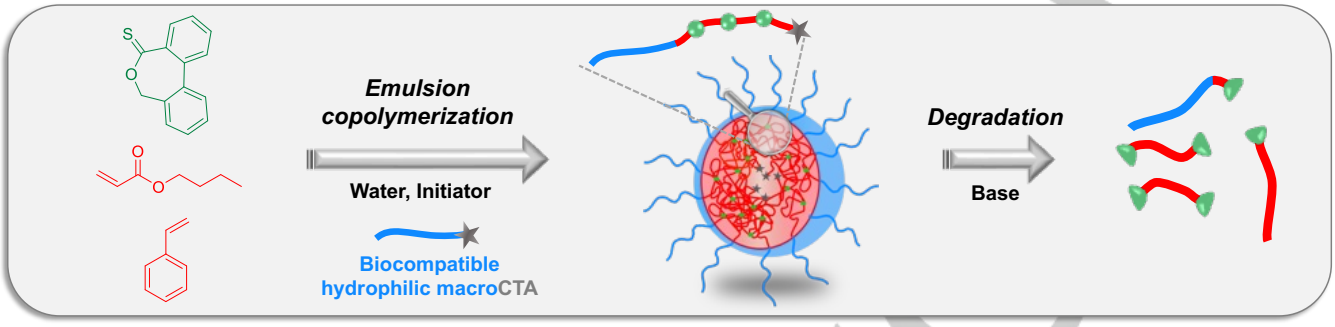

Emulsion copolymerization of dibenzo[c,e]oxepane-5-thione (DOT) with either styrene or *n*-butyl acrylate was carried out in water to produce block copolymer nanoparticles *via* RAFT-mediated PISA in emulsion. Hydrophilic blocks are either poly(*N*-acryloylmorpholine) or poly(ethylene glycol), two polymers largely used for their known biocompatibility. The degradability of the hydrophobic core block is ensured by in-chain cleavable thioester functions.

Institute and/or researcher Twitter usernames: @cp2m_lab; @DAgostoFranck ; @LansalotMuriel